Title

Efficiency fluctuations in quantum thermoelectric devices

Journal

Physical Review B, 91(11)

ISSN

2469-9950

Authors

Esposito, Massimiliano
Ochoa, Maicol A
Galperin, Michael

Publication Date

2015-03-01

DOI

10.1103/physrevb.91.115417

Peer reviewed

Efficiency fluctuations in quantum thermoelectric devices

Massimiliano Esposito
Complex Systems and Statistical Mechanics, Physics and Material Science Research Unit, University of Luxembourg, Luxembourg

Maicol A. Ochoa and Michael Galperin
Department of Chemistry & Biochemistry, University of California San Diego, La Jolla CA 92093, USA
(Dated: February 8, 2015)

We present a method, based on charaterizing efficiency fluctuations, to asses the performance of nanoscale thermoelectric junctions. This method accounts for effects typically arising in small junctions, namely, stochasticity in the junction's performance, quantum effects, and nonequilibrium features preventing a linear response analysis. It is based on a nonequilibrium Green's function (NEGF) approach, which we use to derive the full counting statistics (FCS) for heat and work, and which in turn allows us to calculate the statistical properties of efficiency fluctuations. We simulate the latter for a variety of simple models where our method is exact. By analyzing the discrepancies with the semi-classical prediction of a quantum master equation (QME) approach, we emphasize the quantum nature of efficiency fluctuations for realistic junction parameters. We finally propose an approximate Gaussian method to express efficiency fluctuations in terms of nonequilibrium currents and noises which are experimentally measurable in molecular junctions.

PACS numbers: 05.70.Ln 85.65.+h 85.80.Fi 84.60.Rb

I. INTRODUCTION

The development of thermoelectric materials is at the forefront of the research related to energy conversion and storage. While research on thermoelectricity in bulk materials goes back to the middle of the last century [1], measurements at the nanoscale (and in particular, studies of thermoelectricity in molecular junctions) were only reported recently [2]. The small size of the junctions gives rise to new physical phenomena, not accessible at the macroscopic level, and which are considered promising for reaching more effective energy conversion. The thermoelectric properties of nanoscale junctions have indeed received a lot of attention in the last years, both experimentally [3–14] and theoretically [15–29].

Experimental studies on thermoelectricity in nanoscale junctions make use of the macroscopic theory of thermoelectricity to asses the junction's performance. The latter is characterized by the figure of merit, a quantity exclusively defined in terms of linear response transport coefficients and thus ill-defined out of nonequilibrium. While the linear theory is reasonable in bulk material, it fails in small thermoelectric junctions which can operate in the nonlinear regime (for instance in the resonant tunneling regime). This fact motivated a number of studies to consider the macroscopic efficiency of the junction as an alternative to the figure of merit to characterizes the performance of the junction [30–43]. The macroscopic efficiency is the traditional thermodynamic efficiency of a heat engine defined as the fraction of average power output extracted from the heat arising from the hot source. It is well defined far from equilibrium and upper bounded by the Carnot efficiency.

The nonequilibrium features of the junction are not the only characteristic to be accounted for at the nanoscale. Due to the small size of the system, thermal fluctuations will play a much more import role than in bulk samples, resulting in a high variability in the junction's performance. This variability requires a statistical characterization of the energy conversion which can be performed using the methods of stochastic thermodynamics [44–47]. Such studies have been recently done for small classical energy converters [48–53]. The main idea is to define the efficiency along a single realization of the operating device and to develop techniques to study its fluctuations. Experimental studies of efficiency fluctuation have been very recently performed in Ref. [54].

The third central feature of small thermoelectric junctions which needs to be accounted for are quantum effects. Indeed, quantum coherences can significantly affect charge and energy transfers in molecular junctions as discussed theoretically in Refs [55–60] and shown experimentally in Refs. [61–66].

In this paper we provide a general method to study the performance of nanoscale thermoelectric junctions based on efficiency fluctuations. This methods accounts for the three key features characterizing small junctions, namely, the variability in performance due to fluctuations, operation modes arbitrary far from equilibrium, and quantum effects. It is based on the joint energy and particle full counting statistics (FCS) which we calculate within the nonequilibrium Green's functions (NEGF) formalism. While the quantum FCS of particle currents (e.g. electrons) in junctions is well developed [67–78], that of energy was mostly limited to the quantum master equation (QME) approach [71, 79–84] with its known limitations [76, 85, 86]. By numerically calculating efficiency fluctuations for a set of simple models and comparing our NEGF results with those obtained using a QME approach, we identify the regimes where efficiency

fluctuations display truly quantum features. Moreover, we propose an approximate Gaussian scheme enabling to estimate efficiency fluctuations solely based on experimentally measurable quantities in molecular junctions [87–92], namely the nonequilibrium energy and matter currents and noises.

The structure of the paper is the following. After introducing the FCS of energy, work, and heat within NEGF in Section II, we consider efficiency fluctuations in Section III. In Section IV, we numerically evaluate efficiency fluctuations for various models, compare our results with the QME approach and describe the approximate scheme to estimate efficiency fluctuations experimentally. We summarize our findings in section V.

II. FCS OF PARTICLE AND ENERGY FLUXES

The particle FCS for a single level strongly coupled to Fermi reservoirs was derived in Ref. [69] and generalized to a multilevel interacting system in Ref. [75]. Later, the methodology was applied to describe inelastic transport in junctions in Ref. [77], where the role of quantum coherence on the FCS was discussed.

Here we extend the methodology to count particles and energy in a system strongly coupled to its reservoirs. Similar to the particle FCS [71], the treatment starts by dressing the evolution operator, $\hat{U}(t,t')$ with particle, γ_K^P, and energy, γ_K^E, counting fields at interface K of the junction

$$\hat{U}_\gamma(t,t') = e^{-i\gamma_K^P \hat{N}_K} e^{-i\gamma_K^E \hat{H}_K} \hat{U}(t,t') e^{+i\gamma_K^P \hat{N}_K} e^{+i\gamma_K^E \hat{H}_K} \tag{1}$$

Note that $[\hat{N}_K; \hat{H}_K] = 0$. The counting fields depend on the Keldysh contour branch (see Fig. 1a)

$$\gamma_K = \begin{cases} +\lambda_K^P/2 & \text{at } - \\ -\lambda_K^P/2 & \text{at } + \end{cases} \qquad \gamma_K^E = \begin{cases} +\lambda_K^E/2 & \text{at } - \\ -\lambda_K^E/2 & \text{at } + \end{cases} \tag{2}$$

Here $-$ and $+$ are the time ordered and anti-time ordered branches of the contour, respectively.

Following the procedure outlined in Refs. [69, 77], at steady state we get the following expression for derivatives of the cumulant generating function, $S = -i(t_f - t_i)\,\mathcal{U}$ (here $\mathcal{U}$ is the adiabatic potential), in the counting fields λ_K^M $(M = P, E)$

$$\frac{\partial}{\partial \lambda_K^M} \mathcal{U}(\lambda_K^P, \lambda_K^E) = -\int \frac{dE}{2\pi}\, O_M\, I_K^\lambda(E) \tag{3}$$

where $O_M = 1\,(E)$ for $M = P\,(E)$, and

$$I_K^\lambda(E) \equiv \mathrm{Tr}\Big\{ \mathbf{\Sigma}_K^<(E) e^{i(\lambda_K^P + E\,\lambda_K^E)} \mathbf{G}_\lambda^>(E) - \mathbf{G}_\lambda^<(E) \mathbf{\Sigma}_K^>(E) e^{-i(\lambda_K^P + E\,\lambda_K^E)} \Big\} \tag{4}$$

is the energy resolved dressed particle current at interface K, $\mathrm{Tr}\{\ldots\}$ is the trace over the system subspace,

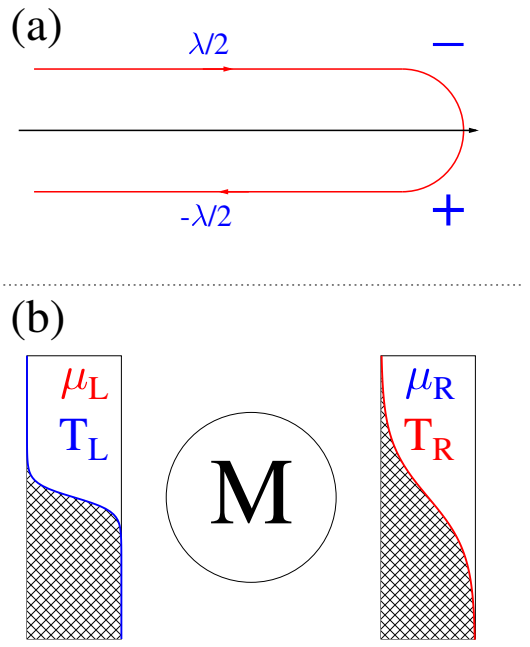

FIG. 1: (Color online) (a) Sketch of the counting field λ dressing of the Keldysh contour forward $(-)$ and backward $(+)$ branches. (b) Sketch of the a nano-thermoelectric junction consisting of a molecule M embedded between two contacts L and R with $T_L < T_R$ and $\mu_L > \mu_R$.

and $G_\lambda^{<(>)}$ is the lesser (greater) projections of the Green function obtained from a counting field dressed version of the Dyson equation (see e.g. Ref. [77] for details).

While the expression for the derivatives of the adiabatic potential in the counting fields can be easily formulated in terms of the field-dressed Green functions and self-energies (see Eq. (3) above or Ref. [77] for a detailed discussion), the corresponding expression for the adiabatic potential itself is more complicated. An explicit expression for the adiabatic potential within the NEGF based particle FCS for a single noninteracting level was derived in Ref. [69]. Exact results for the particle FCS for one-dimensional tight-binding junction models were presented in Ref [72]. Here we consider the case of a multilevel noninteracting system. In particular, we show that for a single level coupled to its reservoirs (and possibly also to other levels with the latter not coupled to reservoirs) or for a multilevel system coupled to reservoirs through single molecular orbitals, the explicit expression for the adiabatic potential in the presence of both particle and energy counting fields is (see Appendix for details)

$$\mathcal{U}\,(\{\lambda\}) = i \int \frac{dE}{2\pi} \ln\Big(1 + \mathcal{T}(E) \times \Big\{ f_L(E)[1 - f_R(E)][e^{+i\left(\lambda_L^P - \lambda_R^P + E(\lambda_L^E - \lambda_R^E)\right)} - 1] + f_R(E)[1 - f_L(E)][e^{-i\left(\lambda_L^P - \lambda_R^P + E(\lambda_L^E - \lambda_R^E)\right)} - 1] \Big\} \Big) \tag{5}$$

where

$$\mathcal{T}(E) \equiv \mathrm{Tr}\{\Gamma_L(E)\, G^r(E)\, \Gamma_R(E)\, G^a(E)\} \tag{6}$$

is the Landauer transmission coefficient at energy E. Here $G^{r(a)}(E)$ are the retarded (advanced) projections of the system Green function in absence of the counting fields, and $\Gamma_K(E)$ is the electron dissipation matrix at energy E due to coupling to contact K ($K = L, R$). The size of the matrix is that of the molecular subspace of the problem. Below we consider systems for which expression (5) is satisfied. In these systems, the electron dissipation rate matrices are always diagonal in the local basis. We denote by Γ_L and Γ_R the parameters characterizing the electron escape rates into the left and right contact, respectively.

The particle and energy average currents and noises can be directly obtained from the adiabatic potential $\mathcal{U}$, Eq. (5), as

$$I_K^M = -\partial_{\lambda_K^M} \mathcal{U}|_{\{\lambda\}=0} \tag{7}$$

$$S_{K_1K_2}^{M_1M_2} = i\, \partial_{\lambda_{K_1}^{M_1}} \partial_{\lambda_{K_2}^{M_2}} \mathcal{U}|_{\{\lambda\}=0}, \tag{8}$$

where $K = L, R$ and $M = P, E$. Explicitly, the average currents read

$$\begin{aligned} I^M &\equiv I_L^M = -I_R^M \\ &= \int \frac{dE}{2\pi}\, O_M\, \mathcal{T}(E)\, [f_L(E) - f_R(E)] \end{aligned} \tag{9}$$

while the noises read

$$\begin{aligned} S^{M_1M_2} &\equiv S_{LL}^{M_1M_2} = S_{RR}^{M_1M_2} = -S_{LR}^{M_1M_2} = -S_{RL}^{M_1M_2} \\ &= S_{shot}^{M_1M_2} + S_{therm}^{M_1M_2}, \end{aligned} \tag{10}$$

where the shot and the thermal (equilibrium) noise respectively read

$$\begin{aligned} S_{shot}^{M_1M_2} &= \int \frac{dE}{2\pi}\, O_{M_1}\, O_{M_2} \\ &\quad \times \mathcal{T}(E)\, (1 - \mathcal{T}(E))\, [f_L(E) - f_R(E)]^2 \end{aligned} \tag{11}$$

$$\begin{aligned} S_{therm}^{M_1M_2} &= \sum_{K=L,R} \int \frac{dE}{2\pi}\, O_{M_1}\, O_{M_2} \\ &\quad \times \mathcal{T}(E)\, f_K(E)\, [1 - f_K(E)]\,. \end{aligned} \tag{12}$$

Expressions (7)-(12) are exact for any non-interacting system bi-linearly coupled to two contacts.

III. EFFICIENCY FLUCTUATION

In order to operate as a thermoelectric junction the small quantum system is embedded between two leads L and R with $T_L < T_R$ and $\mu_L > \mu_R$ (see Fig. 1b). The macroscopic efficiency of such a junction is defined as the ratio between the average power generated by the device, $\dot{W} = (\mu_L - \mu_R) I^P$, and the average heat taken from the hot reservoir which fuels the device, $\dot{Q} = -(I^E - \mu_R I^P)$, namely $\bar{\eta} = \dot{W}/\dot{Q}$. It is upper bounded by the Carnot efficiency $\bar{\eta} \leq 1 - T_L/T_R$. The fluctuating efficiency on the other hand is defined as the ratio between the fluctuation power w/t and heat flow q/t measured at the level of a single experiential realization of duration t, namely $\eta = w/q$. Efficiency fluctuations are not bounded and are characterized by the rate $J(\eta)$ at which the probability to observe a given efficiency η decays during a long measurement realization [48, 49]

$$P(\eta) \overset{t\to\infty}{=} \exp\{-J(\eta)t\}. \tag{13}$$

This rate is called the large deviation function (LDF) of efficiency. It can be derived from the heat and work FCS obtained from the energy and heat FCS (5) as follows. The heat entering the system from the hot (cold) reservoir is given by the right (left) energy current minus μ_R (μ_L) times the right (left) particle current. At steady-state, the particle and energy currents are equal (but with opposite signs) at the two interfaces. Therefore, by the first law of thermodynamics, the work generated by the particles moving across the system is equal to the sum of the heat from the left and right reservoir which is thus $\mu_R - \mu_L$ multiplied by the right particle current. This means that if λ_Q counts the heat from the hot reservoir and if λ_W counts the work, we get that the heat and work FCS reads

$$\begin{aligned} \mathcal{U} = i \int \frac{dE}{2\pi} \ln \Big(& 1 + T(E) \\ & \times \Big\{ f_L(E)[1 - f_R(E)][e^{-i([E-\mu_R]\lambda_Q - [\mu_L - \mu_R]\lambda_W)} - 1] \\ & + f_R(E)[1 - f_L(E)][e^{+i([E-\mu_R]\lambda_Q - [\mu_L - \mu_R]\lambda_W)} - 1] \Big\} \Big). \end{aligned} \tag{14}$$

Introducing the slightly modified version of the adiabatic potential, $\phi \equiv -i\mathcal{U}$, and redefining the counting fields as $\gamma \equiv i\lambda_W$ and $\lambda \equiv i\lambda_Q$, we get that

$$\begin{aligned} \phi(\gamma, \lambda) = \int \frac{dE}{2\pi} \ln \Big(& 1 + T(E) \\ & \times \Big\{ f_L(E)[1 - f_R(E)][e^{-([E-\mu_R]\lambda - [\mu_L - \mu_R]\gamma)} - 1] \\ & + f_R(E)[1 - f_L(E)][e^{+([E-\mu_R]\lambda - [\mu_L - \mu_R]\gamma)} - 1] \Big\} \Big). \end{aligned} \tag{15}$$

Note that the fluctuation theorem symmetry holds

$$\phi\Big(\gamma, \lambda\Big) = \phi\Big(-\frac{1}{T_L} - \gamma, \frac{1}{T_R} - \frac{1}{T_L} - \lambda \Big) \tag{16}$$

as can be verified using the property

$$\begin{aligned} & f_R(E)[1 - f_L(E)] e^{\left([E-\mu_R](\frac{1}{T_R} - \frac{1}{T_L} - \lambda) - [\mu_L - \mu_R](-\frac{1}{T_L} - \gamma)\right)} \\ & = f_R(E)[1 - f_L(E)] e^{-\frac{E-\mu_L}{T_L} + \frac{E-\mu_R}{T_R}}\, e^{-([E-\mu_R]\lambda - [\mu_L - \mu_R]\gamma)} \\ & \equiv f_L(E)[1 - f_R(E)] e^{-([E-\mu_R]\lambda - [\mu_L - \mu_R]\gamma)}. \end{aligned} \tag{17}$$

The efficiency LDF is finally obtain by setting $\lambda = \eta\gamma$ and minimizing ϕ relative to the field γ, namely [48, 49]

$$J(\eta) = -\min_{\gamma} \phi(\gamma, \eta\gamma). \tag{18}$$

The convexity of (15) together with the fluctuation theorem symmetry (16) has been used in classical systems to prove two important results. First, the single minimum in $J(\eta)$ (i.e. the most probable efficiency) corresponds to the macroscopic efficiency $\bar{\eta}$, second, the single maximum in $J(\eta)$ (i.e. the least likely efficiency) corresponds to the Carnot efficiency $1 - T_L/T_R$ [48, 49]. By showing that the fluctuation theorem symmetry (16) holds for the adiabatic potential of quantum junctions, we thus generalized these remarkable results to the quantum realm.

In the limit of weak system-lead coupling, $\Gamma \equiv \Gamma_L + \Gamma_R \to 0$, Eq. (15) reduces to the QME approach prediction [71, 93]

$$\phi(\gamma,\lambda) = \tag{19}$$
$$\sum_s \Bigg(-\frac{\Gamma_s(E_s)}{2} + \Bigg[\left(\frac{\Gamma_s(E_s)}{2}\right)^2 + \Gamma_s^L(E_s)\Gamma_s^R(E_s)$$
$$\times \Big\{ f_L(E_s)[1-f_R(E_s)][e^{-([E_s-\mu_R]\lambda-[\mu_L-\mu_R]\gamma)} - 1]$$
$$+ f_R(E_s)[1-f_L(E_s)][e^{+([E_s-\mu_R]\lambda-[\mu_L-\mu_R]\gamma)} - 1] \Big\} \Bigg]^{1/2} \Bigg).$$

Here $\sum_s \ldots$ is the sum over the eigenorbitals of the system with eigenenergies E_s, and $\Gamma_s(E_s) \equiv \Gamma_s^L(E_s) + \Gamma_s^R(E_s)$ is the total escape rate from the eigenorbital s evaluated at energy of the the orbital. The quasi-classical nature of this result is manifest since Eq. (19) disregards the reservoir induced correlations between the eigenorbitals of the system. This form of adiabatic potential was used in Refs. [48, 49] together with (18) to calculate efficiency fluctuations in a photoelectric device.

IV. NUMERICAL EXAMPLES

We now compare the efficiency fluctuations (18) predicted using the NEGF heat and work FCS (15) with the QME prediction (19). Since we exclusively consider non-interacting models, we emphasize that the NEGF treatment is exact while the QME approach is an approximate approach only valid in the weak coupling limit to the contact and which neglects coherences between system eigenstates (we use the rotating wave approximation to guarantee positivity). The discrepancies between these two approaches can thus be attributed to broadening effects induced by strong coupling and to eigenbasis coherences.

The calculations are performed by numerically evaluating the adiabatic potential $\phi(\gamma, \eta\gamma)$ (using Eq.(15) for the NEGF and Eq.(19) for the QME) and numerically minimizing it as a function of the counting field γ for a fixed value of the efficiency η according to Eq.(18).

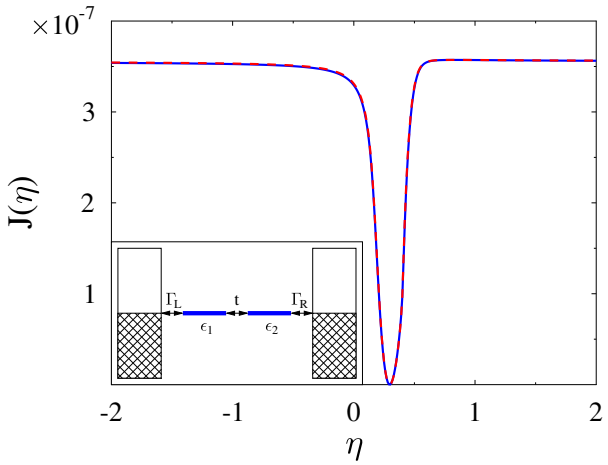

FIG. 2: (Color online) Efficiency LDF for a two-level bridge calculated within the NEGF (solid line, blue) and the QME (dashed line, red) approaches. See text for parameters.

Unless specified otherwise, the parameters of the calculations are $T_L = 100$ K, $T_R = 600$ K, $\mu_L = 0.02$ eV and $\mu_R = 0$. We use the wide band approximation which assumes that the electron escape rates Γ_L and Γ_R are energy-independent constants. The NEGF calculations were performed on an energy grid spanning the region from -1 to 1 eV with step 10^{-5} eV.

We start by considering the two-level bridge model depicted in inset in Fig. 2 when the system is weakly coupled to the contacts. The position of the levels is $\varepsilon_1 = \varepsilon_2 = 0.1$ eV, the electron hopping parameter is $t = 0.05$ eV, and the electron escape rates are $\Gamma_L = \Gamma_R = 2 \cdot 10^{-4}$ eV. As expected, in this regime both the NEGF and the QME predictions for the efficiency fluctuation coincide (compare the solid and the dashed lines in Fig. 2). Large values of $J(\eta)$ indicates unlikely efficiency fluctuations while the minimum is the most likely efficiency $\bar{\eta}$ corresponding to the macroscopic efficiency considered in traditional thermodynamics. Although hardly seen on this figure, the most unlikely efficiency is located at the Carnot efficiency $1 - T_L/T_R \approx 0.83$. The probability distribution in this regime is thus quite narrowly centered around the most likely efficiency.

We consider two types of junctions, a two-level bridge (top inset in Fig. 3) and a single level junction coupled to an isolated orbital (bottom inset in Fig. 3). Both junctions are in regimes where the system is strongly coupled to the contacts. The latter is the simplest model often used to describe destructive interference effect in transport through a junction (see e.g. Ref. [76]). The position of the levels is $\varepsilon_1 = \varepsilon_2 = 0.12$ eV, the electron hopping parameter is $t = 0.05$ eV, and the electron escape rates are $\Gamma_L = \Gamma_R = 0.1$ eV. Figure 3a shows that QME results of the two models are identical. This result stems from the fact that in the rotating wave approximation, the QME neglects coherences in the system eigenbasis

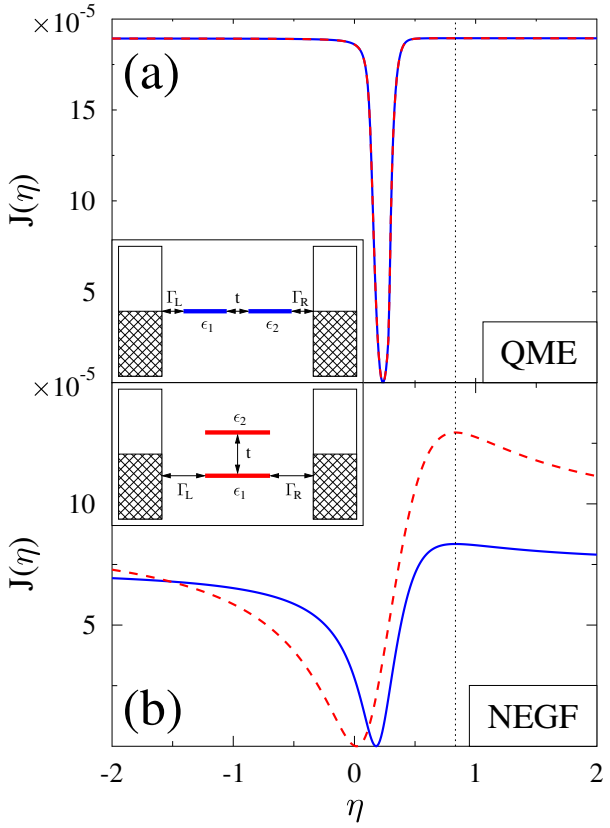

FIG. 3: (Color online) Efficiency LDF for a two-level bridge (top inset; solid line, blue) and a single level coupled to an isolated orbital (bottom inset; dashed line, red), calculated within the (a) QME and (b) NEGF approaches. The vertical dashed line shows the Carnot efficiency. See text for parameters.

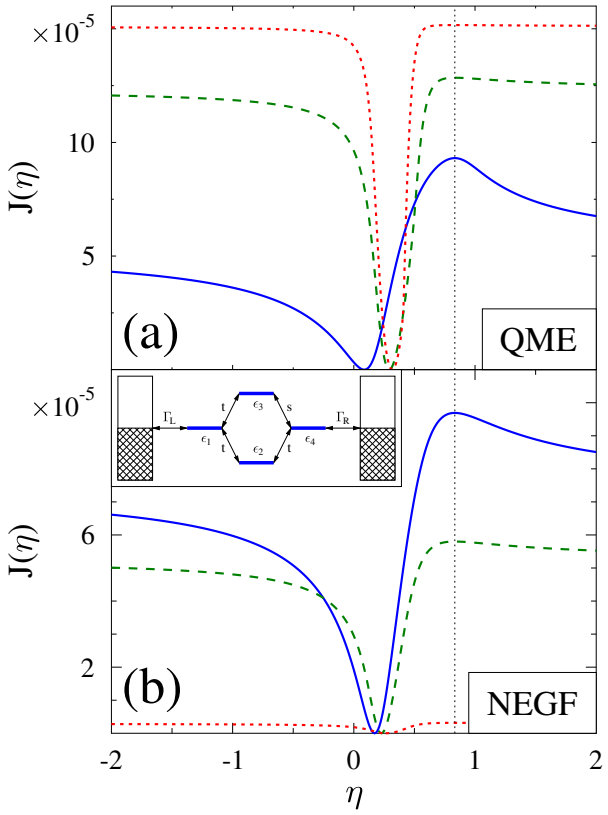

FIG. 4: (Color online) Efficiency LDF for a donor-bridge-acceptor junction calculated within the (a) QME and (b) NEGF approaches. Results are shown for constructive interference ($s = t$; solid line, blue), single path ($s = 0$; dashed line, green), and destructive interference ($s = -0.8\,t$; dotted line, red). The vertical dashed line shows the Carnot efficiency. Other parameters are as in Fig. 3.

[76, 86]. Fig. 3b shows the exact efficiency fluctuations for the two models. The interference effects responsible for the discrepancy between the two curves do not significantly alter the qualitative shape of the efficiency LDF. However, when comparing Figs. 3a and b, we note that the broadening effects resulting from the strong coupling to the contacts clearly tend to increase the magnitude of the efficiency fluctuations and also intensifies the asymmetry of the fluctuations around the most likely value. We note that even the most likely value is affected. The least likely value is nevertheless still exactly located at the Carnot efficiency.

We now turn to the donor-bridge-acceptor (DBA) junction depicted in the inset of Fig. 4. This setup enables to study the effect of intra-molecular interference on efficiency fluctuations. We see that the trend predicted by the QME, when moving from constructive to destructive interference (solid to dashed to dotted line), is the opposite of the real trend obtained using the exact NEGF. It is interesting to observe that destructive interference tend to increase the most likely efficiency but at the same time significantly increase the magnitude of the efficiency fluctuations. In other words, the performance of the junction increases but at the cost of becoming less reproducible.

As a final example we consider a single level junction (see inset in Fig. 5). Within the QME approach, the efficiency does not fluctuate in this model because heat and work are directly proportional to each other, a condition known as tight coupling [50]. However, the NEGF approach breaks the tight coupling condition due to the hybridization of the molecular level with the states in the contacts. The position of the level is taken as $\varepsilon = 0.1$ eV and Figure 5 shows the results of calculations for several strengths of the system-reservoir coupling: $\Gamma_L = \Gamma_R = 0.1$ eV (solid line), 0.05 eV (dashed line), 0.01 eV (dash-dotted line), and 0.001 eV (dotted line). As $\Gamma \to 0$ (weak coupling limit) the distribution becomes very narrow and centered around the macroscopic efficiency $(\mu_L - \mu_R)/(\varepsilon - \mu_R)$.

We now discuss ways to relate the efficiency LDF to experimentally measurable characteristics of the junction. For the setup sketched in Fig. 1b, the average power and

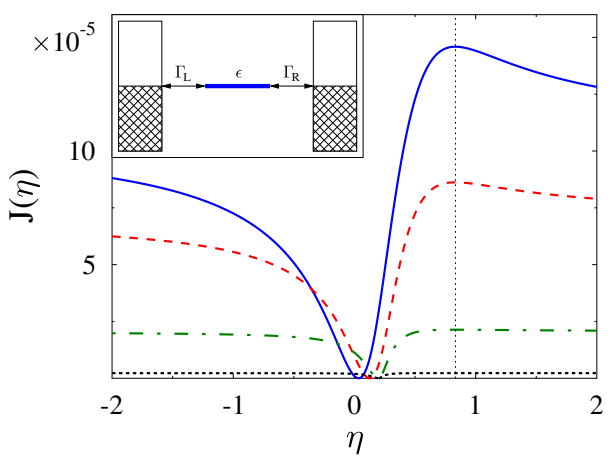

FIG. 5: (Color online) Efficiency LDF calculated within the NEGF for a single level junction. The results are shown for several level-contacts coupling strengths ranging from the strongest (solid line, blue) to the weakest (dotted line, black). The vertical dashed line shows the Carnot efficiency. See text for parameters.

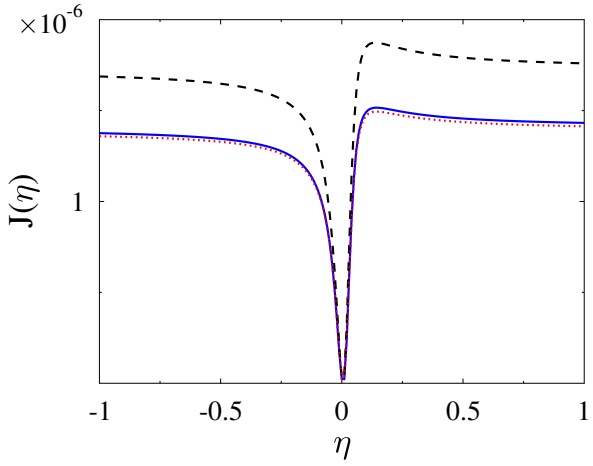

FIG. 6: (Color online) Efficiency LDF for a single level junction (see inset in Fig. 5) calculated for experimentally relevant parameters. The predictions of the exact NEGF calculations (solid line, blue) are compared to the linear response predictions (29) (dashed line, black), and to the Gaussian approximation predictions (33) (dotted line, red). See text for parameters.

the heat flux from the hot reservoir are

$$\dot{W} = \Delta\mu\, I^P \tag{20}$$

$$\dot{Q} = -\left(I^E - \mu_R\, I^P\right), \tag{21}$$

where I^P and I^E are defined in Eq. (9) and $\Delta\mu \equiv \mu_L - \mu_R$. In the linear response regime (obtained by linearizing the Fermi distributions in $1/T_{L(R)}$ and $\mu_{L(R)}/T_{L(R)}$ around equilibrium $\mu_L = \mu_R = E_F$ and $T_L = T_R = T$), we get that

$$\dot{W} \approx G\,\Delta\mu^2 + L\,\Delta\mu\,\Delta\beta \tag{22}$$

$$\dot{Q} \approx R\,\Delta\mu + F\,\Delta\beta \tag{23}$$

where $\Delta\beta = 1/T_L - 1/T_R$ and

$$G = -\int \frac{dE}{2\pi}\,\mathcal{T}(E)\,f'(E)\,\frac{1}{T_L} \tag{24}$$

$$L = \int \frac{dE}{2\pi}\,\mathcal{T}(E)\,f'(E)\,(E-\mu_R) \tag{25}$$

$$R = \int \frac{dE}{2\pi}\,\mathcal{T}(E)\,f'(E)\,\frac{E-\mu_R}{T_L} \tag{26}$$

$$F = -\int \frac{dE}{2\pi}\,\mathcal{T}(E)\,f'(E)\,(E-\mu_R)^2. \tag{27}$$

Here $f'(E) = [d/dx\, 1/(e^x+1)]_{x=(E-E_F)/T}$ and $R = L/T_L$. The coefficients in (24) are related to experimentally measurable quantities. Indeed, G is the electrical conductance, and if κ denotes the heat conductance and S the Seebeck coefficient, we have that

$$\kappa = \frac{F}{T_L\,T_R}; \qquad S = \frac{L}{G\,T_L\,T_R}. \tag{28}$$

Thus following Ref. [48], in the linear response regime the efficiency LDF can be expressed in terms of these measurable quantities as

$$J(\eta) = \frac{\left[\eta(\kappa\,\Delta T + G\,S\,T_R\,\Delta\mu) + G\,S\,\Delta T\Delta\mu + G\,\Delta\mu^2\right]^2}{4\left[\eta^2\,\kappa\,T_L\,T_R + 2\,\eta\,G\,S\,T_L\,T_R\,\Delta\mu + G\,T_L\,\Delta\mu^2\right]}, \tag{29}$$

where $\Delta T = T_R - T_L$.

We now attempt to estimate the efficiency LDF beyond the linear regime, solely in terms of the particle and energy nonequilibrium currents and noises, Eqs. (9)-(12). Note that in molecular junctions, the particle and energy currents as well as the particle noise are experimentally measurable [87–89, 91] and the energy noise will soon become measurable [94–96]. To do so, we approximate the cumulant generating function (15) by a quadratic expansion in counting fields γ and λ around point $\gamma = \lambda = 0$. This is a Gaussian assumption which leads to

$$\phi(\gamma, \eta\gamma) \approx a\gamma^2 + b\gamma, \tag{30}$$

where we used the fact that $\phi(0,0) = 0$, and defined

$$a \equiv \frac{\eta^2}{2}S^{EE} + \frac{(\mu_L - \mu_R[1-\eta])^2}{2}S^{PP} - \eta\,(\mu_L - \mu_R[1-\eta])\,S^{PE} \tag{31}$$

$$b \equiv -\,\eta\,I^E + (\mu_L - \mu_R[1-\eta])\,I^P, \tag{32}$$

which are solely expressed in terms of the measurable nonequilibrium particle and energy fluxes, Eq. (9), and of the nonequilibrium noise characteristics of the junction (10). Within this Gaussian approximation, we find that

$$J(\eta) = \frac{b^2}{4\,a}. \tag{33}$$

We have thus shown that efficiency fluctuations are experimentally measurable close to equilibrium (29) and in the Gaussian approximation (33). We now verify the validity of these approximations in Fig. 6 where the exact efficiency LDF, Eqs. (15) and (18), is compared to the linear response, Eq. (29), and the Gaussian approximation, Eq. (33), result for an experimentally relevant set of parameters: $T_L = 300$ K, $T_R = 350$ K, $\mu_L = 0.002$ eV, $\mu_R = 0$ [3]. We also set $\varepsilon = 0.1$ eV and $\Gamma_L = \Gamma_R = 0.1$ eV. We see that near the minimum corresponding to the macroscopic efficiency, the three curves coincide (thus justifying the use of linear response to estimates of average quantities). At the same time, the efficiency fluctuations are poorly captured by the linear response approximation (dashed line) but reproduced quite well by the Gaussian approximation (dotted line).

V. CONCLUSION

We studied the thermoelectric properties of nanoscale junctions. Since stochasticity and quantum coherence are expected to be important at small scale, we proposed to characterize the performance of these devices by studying efficiency fluctuations rather than the widely used figure of merit which is intrinsically restricted to the linear regime. We provided a systematic procedure to study efficiency fluctuations which accounts for all quantum effects and is based on the work and heat FCS obtained within the NEGF formalism. As predicted for classical dynamics in Ref. [48], the most likely efficiency coincides with the macroscopic efficiency, while the least likely efficiency corresponds to the Carnot efficiency. We used simple models with realistic molecular junction parameters to compare our NEGF based method to the commonly used QME approach. We showed that the latter may fail qualitatively for strong system-reservoir coupling due to its inability to properly account for quantum coherences in the system. We finally proposed a method to estimate efficiency fluctuations using the experimentally measurable particle and energy nonequilibrium currents and noises. Linear response and Gaussian approximations were proposed as ways to construct efficiency fluctuations from experimental measurements. We showed that while linear response approach, often used in the experimental literature to discuss thermoelectric properties of junctions, captures the macroscopic efficiency, it fails to account for the efficiency fluctuations. At the same time, the Gaussian approximation was shown to work very well within experimentally relevant range of parameters.

Acknowledgments

M.E. is supported by the National Research Fund, Luxembourg in the frame of project FNR/A11/02. M.G. gratefully acknowledges support by the Department of Energy (Early Career Award, DE-SC0006422).

Appendix A: Cumulant generating function of a multilevel non-interacting system

Here we derive the general form of the adiabatic potential $\mathcal{U}(\lambda)$ for a noninteracting n-level system. For simplicity, we consider the specific case of one particle counting field λ in the left molecule-contact interface. Multiple counting fields and/or energy FCS are formulated similarly. We first find expression for the potential derivative in the counting field, Eqs. (3) and (7), and then integrate it in the field to get the potential itself.

We start by writing the dressed Green Function $G(\lambda)$ as a $2n \times 2n$ dimensional block matrix in the Keldysh contour

$$G(\lambda) = \begin{bmatrix} G^c_\lambda & G^<_\lambda \\ G^>_\lambda & G^{\tilde{c}}_\lambda \end{bmatrix}, \tag{A1}$$

inverse of which is [69]

$$G^{-1}(\lambda) = \begin{bmatrix} -i\Gamma_L(f_L(E)-1/2) - i\Gamma_R(f_R(E)-1/2) + IE - H_M & ie^{i\lambda}\Gamma_L f_L(E) + i\Gamma_R f_R(E) \\ -ie^{-i\lambda}\Gamma_L(1-f_L(E)) - i\Gamma_R(1-f_R(E)) & -i\Gamma_L(f_L(E)-1/2) - i\Gamma_R(f_R(E)-1/2) - IE + H_M \end{bmatrix}. \tag{A2}$$

We will use Jacobi's formula for the derivative of the determinant of a matrix that in our case reads

$$\frac{d}{d\lambda}\det(G^{-1}(\lambda)) = \mathrm{Tr}\left\{\mathrm{adj}\left(G^{-1}(\lambda)\right)\frac{d}{d\lambda}G^{-1}(\lambda)\right\}, \tag{A3}$$

where $\mathrm{adj}(M)$ denotes the adjugate matrix of a matrix M ($\mathrm{adj}(M)M = I\det(M) = M\,\mathrm{adj}(M)$). For our consideration, it will be important to work with special submatrices of G^{-1}. For an $n \times n$ matrix M, we define $M(j|i)$ to be the $(n-1)\times(n-1)$ matrix that is obtained from M by removing the jth row and the ith column. In this notation

the (i,j)-matrix element for the adjugate of M can be expressed as $\mathrm{adj}(M)_{ij} = (-1)^{i+j}\det(M(j|i))$. Also below $M[j_1\dots j_r|i_1\dots i_r]$ will denote the submatrix of M composed of rows $j_1\dots j_r$ and columns $i_1\dots i_r$.

The first step in the derivation is to obtain from Eq. (A2)

$$\frac{d}{d\lambda}G^{-1}(\lambda) = \begin{bmatrix} 0 & -e^{i\lambda}\Gamma_L f_L(E) \\ -e^{-i\lambda}\Gamma_L(1-f_L(E)) & 0 \end{bmatrix}, \tag{A4}$$

and utilizing Eq. (A3) calculate

$$\begin{aligned}
\frac{1}{\det(G^{-1}(\lambda))}\frac{d}{d\lambda}\det(G^{-1}(\lambda)) =& \frac{1}{\det(G^{-1}(\lambda))}\mathrm{Tr}\left\{\mathrm{adj}\left(G^{-1}(\lambda)\right)\frac{d}{d\lambda}G^{-1}(\lambda)\right\} \\
=& \mathrm{Tr}\left\{\frac{\mathrm{adj}\left(G^{-1}(\lambda)\right)}{\det(G^{-1}(\lambda))}\begin{bmatrix} 0 & -e^{i\lambda}\Gamma_L f_L(E) \\ -e^{-i\lambda}\Gamma_L(1-f_L(E)) & 0 \end{bmatrix}\right\} \\
=& \mathrm{Tr}\left\{\begin{bmatrix} G^c_\lambda(E) & G^<_\lambda(E) \\ G^>_\lambda(E) & G^{\tilde{c}}_\lambda(E) \end{bmatrix}\begin{bmatrix} 0 & -e^{i\lambda}\Gamma_L f_L(E) \\ -e^{-i\lambda}\Gamma_L(1-f_L(E)) & 0 \end{bmatrix}\right\} \\
=& \mathrm{Tr}\left\{G^<_\lambda(E)(-e^{-i\lambda})\Gamma_L(1-f_L(E)) + G^>_\lambda(E)(-e^{i\lambda})\Gamma_L f_L(E)\right\} \\
=& iI^\lambda_L(E).
\end{aligned} \tag{A5}$$

Using this last result in Eq.(3) and integrating with respect to the counting field λ leads to

$$\mathcal{U}(\lambda) = i\int\frac{dE}{2\pi}\ln\left[\frac{\det(G^{-1}(\lambda))}{\det(G^{-1}(0))}\right]. \tag{A6}$$

where we used the known property $\mathcal{U}(0) = 0$. Eq. (A6) is the first important result.

We now have to evaluate the determinants inside the logarithm in Eq. (A6). The determinants can be evaluated after applying elementary transformations to G^{-1}. First, we notice that we can write

$$\det(G^{-1}(\lambda)) = \begin{vmatrix} -\Sigma^>(E) + G^{a,-1} & -i(1-e^{i\lambda})\Gamma_L f_L(E) + \Sigma^<(E) \\ i(1-e^{-i\lambda})\Gamma_L(1-f_L(E)) + \Sigma^>(E) & -G^{r,-1} - \Sigma^>(E) \end{vmatrix}, \tag{A7}$$

where $G^{r,-1} = IE - H_M + i(\Gamma_L+\Gamma_R)/2$ and $G^{a,-1} = (G^{r,-1})^\dagger$, by adding and subtracting to each submatrix in Eq. (A2) appropriate matrices. Then we add to the i-th row, $i \le n$ the $(n+i)$th row of the matrix. After which, on the resulting matrix, we add the $(n+j)$-th column to the j-th column for each $j \le n$. This leads to

$$\det(G^{-1}(\lambda)) = \begin{vmatrix} i(1-e^{-i\lambda})\Gamma_L(1-f_L(E)) + G^{a,-1} & -i(1-e^{i\lambda})\Gamma_L f_L(E) + i(1-e^{-i\lambda})(1-f_L(E))\Gamma_L \\ i(1-e^{-i\lambda})\Gamma_L(1-f_L(E)) + \Sigma^>(E) & i(1-e^{-i\lambda})\Gamma_L(1-f_L(E)) - G^{r,-1} \end{vmatrix} \tag{A8}$$

Setting $\lambda = 0$ we arrive at the result for the first of the determinants in Eq. (A6)

$$\det(G^{-1}(0)) = \det(G^{a,-1})\det(-G^{r,-1}), \tag{A9}$$

To get the second determinant in Eq. (A6) we have to work with the general form of Eq. (A7). Explicit evaluations lead to an expression that can be grouped in powers of $(1-e^{-i\lambda})$ and $(1-e^{i\lambda})$ of at most n power. In particular, noticing that $(1-e^{-i\lambda})(1-e^{i\lambda}) = (1-e^{-i\lambda}) + (1-e^{i\lambda})$ we can write

$$\det(G^{-1}(\lambda)) = \det(G^{a,-1})\det(-G^{r,-1}) + \sum_{s=1}^{n}(1-e^{-i\lambda})^s a_s + (1-e^{i\lambda})^s b_s, \tag{A10}$$

where a_s and b_s are the coefficients of the polynomial given by [97]

$$a_s = (i)^s(1-f_L(E))^s\sum_{\alpha\in Q_{s,n}}\sum_{\beta\in Q_{s,n}}(-1)^{\sigma(\alpha+n)+\sigma(\beta)}\det(\Gamma_L[\alpha|\beta])\det(N(\alpha+n|\beta)) \tag{A11}$$

$$b_s = (-i)^s(f_L(E))^s\sum_{\alpha\in Q_{s,n}}\sum_{\beta\in Q_{s,n}}(-1)^{\sigma(\alpha)+\sigma(\beta+n)}\det(\Gamma_L[\alpha|\beta])\det(M(\alpha|\beta+n)) \tag{A12}$$

where N and M are $2n\times 2n$ matrices given by

$$N = \begin{bmatrix} -\Sigma^>(E) + G^{a,-1} & i\Gamma_R f_R(E) \\ \Sigma^>(E) & -G^{r,-1} - \Sigma^>(E) \end{bmatrix}, \qquad M = \begin{bmatrix} -\Sigma^>(E) + G^{a,-1} & \Sigma^<(E) \\ -i\Gamma_R(1-f_R(E)) & -G^{r,-1} - \Sigma^>(E) \end{bmatrix}, \tag{A13}$$

$Q_{s,n}$ is the set of s-tuples $(i_1,\ldots,i_s)$ of natural numbers such that $1 \le i_1 < i_2 < \cdots < i_{s-1} < i_s \le n$, $\sigma(\alpha) = \sum \alpha_i$ for $\alpha \in Q_{s,n}$, and $\alpha + n = (\alpha_1 + n, \alpha_2 + n, \ldots, \alpha_s + n)$. From equations (A11) and (A12) we have in particular $a_n = ((1 - f_L(E))f_R(E))^n \det(\Gamma_L\Gamma_R)$ and $b_n = ((1 - f_R(E))f_L(E))^n \det(\Gamma_L\Gamma_R)$. Eqs. (A10)-(A12) give the most general form for the second determinant in Eq. (A6).

Finally, substituting Eqs. (A9) and (A10) into (A6) we obtain the general form for the adiabatic potential

$$\mathcal{U}(\lambda) = i \int \frac{dE}{2\pi} \ln\left[1 + \sum_{s=1}^{n} \frac{a_s\,(1 - e^{-i\lambda})^s}{\det(G^{a,-1})\det(-G^{r,-1})} + \frac{b_s\,(1 - e^{i\lambda})^s}{\det(G^{a,-1})\det(-G^{r,-1})}\right], \tag{A14}$$

with the coeffcients a_s and b_s given by Eqs. (A11) and (A12).

We now consider two specific examples where we can recover the expression derived in Ref. [69] for a single level junction from our general result, Eq. (A14).

1. **One level**.
   By direct computation of Eqs. (A11) and (A12) we find

   $$a_1 = \Gamma_L\Gamma_R(1 - f_L(E))f_R(E) \qquad\qquad b_1 = \Gamma_L\Gamma_R(1 - f_R(E))f_L(E).$$

   Thus

   $$\begin{aligned}\frac{\det(G^{-1}(\lambda))}{\det(G^{-1}(0))} =& 1 + \frac{\Gamma_R\Gamma_L}{G^{a,-1}(-G^{r,-1})}\left((1 - e^{-i\lambda})(1 - f_L(E))f_R(E) + (1 - e^{i\lambda})(1 - f_R(E))f_L(E)\right)\\ =& 1 + G^r(E)\Gamma_R G^a(E)\Gamma_L\left((e^{i\lambda} - 1)(1 - f_L(E))f_R(E) + (e^{-i\lambda} - 1)(1 - f_L(E))f_R(E)\right)\end{aligned}$$

   which yields the expression for adiabatic potential derived in Ref. [69].

2. **n-level system coupled to the contacts through single orbitals.**
   In this case Γ_L and Γ_R are $n \times n$ matrices with all entries equal zero but one element in the diagonal. Examples of systems of this kind are the two level bridge (see inset in Fig. 2) or D-B-A type of the junction (see inset in Fig. 4). Here we can take $[\Gamma_L]_{ij} = \delta_{1j}\delta_{i1}\gamma_L$ and $[\Gamma_R]_{ij} = \delta_{nj}\delta_{in}\gamma_R$, which results in $a_s = b_s = 0$ for $s > 1$ and

   $$\begin{aligned} a_1 =& i(1 - f_L(E))(-1)^{1+n+1}\det(\Gamma_L[1|1])\det(N(1+n|1))\\ =& i(1 - f_L(E))(-1)^n\gamma_L\begin{vmatrix} -\Sigma^{>}(|1)(E) + G^{a,-1}(|1) & i\Gamma_R f_R(E) \\ -i\Gamma_R(1|1)(1 - f_R(E)) & -G^{r,-1}(1|) - \Sigma^{>}(1|)(E)\end{vmatrix}\\ =& i(1 - f_L(E))(-1)^n\gamma_L(-1)^{n+2n-1}i\gamma_R f_R(E)\begin{vmatrix} -\Sigma^{>}(n|1)(E) + G^{a,-1}(n|1) & 0 \\ -i\Gamma_R(1|1)(1 - f_R(E)) & -G^{r,-1}(1|n) - \Sigma^{>}(1|n)(E)\end{vmatrix}\\ =& (1 - f_L(E))f_R(E)\gamma_L\gamma_R\det(G^{a,-1}(n|1))\det(-G^{r,-1}(1|n)) \end{aligned} \tag{A15}$$

   where we used $\Sigma^{>}(n|1)(E) = \Sigma^{>}(1|n)(E) = 0$. Similarly

   $$b_1 = f_L(E)(1 - f_R(E))\gamma_L\gamma_R\det(G^{a,-1}(1|n))\det(-G^{r,-1}(n|1)). \tag{A16}$$

   From the definition of the adjugate we have $(-1)^{1+n}\det(G^{a,-1}(1|n)) = \mathrm{adj}(G^{a,-1})_{n1}$, $(-1)^{n+1}\det(-G^{r,-1}(n|1)) = \mathrm{adj}(-G^{r,-1})_{1n}$. Also in this particular case $\mathrm{adj}(G^{a,-1})_{1n} = \mathrm{adj}(G^{r,-1})_{1n}$ and $\mathrm{adj}(G^{a,-1})_{n1} = \mathrm{adj}(G^{r,-1})_{n1}$. Finally, substituting Eqs. (A15) and (A16) into Eq. (A14) and rearranging terms, we get

   $$\begin{aligned}\mathcal{U}(\lambda) =& i\int \frac{dE}{2\pi}\ln\Big[1 + \mathrm{Tr}\{G^r(E)\Gamma_R G^a(E)\Gamma_L\}\\ &\times\left((e^{i\lambda} - 1)(1 - f_L(E))f_R(E) + (e^{-i\lambda} - 1)(1 - f_L(E))f_R(E)\right)\Big]\end{aligned} \tag{A17}$$

   Eq. (A17) is the Levitov-Lesovik formula for a multi-level system.

[1] A. F. Ioffe, *Semiconductor Thermoelements and Thermoelectric Cooling* (Infosearch Ltd., London, 1957).

[2] P. Kim, L. Shi, A. Majumdar, and P. L. McEuen, Phys.

Rev. Lett. **87**, 215502 (2001).
[3] P. Reddy, S.-Y. Jang, R. A. Segalman, and A. Majumdar, Science **315**, 1568 (2007).
[4] H. Park, Nature Mater. **6**, 330 (2007).
[5] J. A. Malen, S. K. Yee, A. Majumdar, and R. A. Segalman, Chem. Phys. Lett. **491**, 109 (2010).
[6] J. R. Widawsky, P. Darancet, J. B. Neaton, and L. Venkataraman, Nano Letters **12**, 354 (2012).
[7] M. D. Losego, M. E. Grady, N. R. Sottos, D. G. Cahill, and P. V. Braun, Nat Mater **11**, 502 (2012).
[8] W. C. Germs, K. Guo, R. A. J. Janssen, and M. Kemerink, Phys. Rev. Lett. **109**, 016601 (2012).
[9] M. Tsutsui, T. Morikawa, A. Arima, and M. Taniguchi, Sci. Rep. **3**, 3326 (2013).
[10] W. Lee, K. Kim, W. Jeong, L. A. Zotti, F. Pauly, J. C. Cuevas, and P. Reddy, Nature **498**, 209 (2013).
[11] J.-P. Brantut, C. Grenier, J. Meineke, D. Stadler, S. Krinner, C. Kollath, T. Esslinger, and A. Georges, Science **342**, 713 (2013).
[12] M. Chabinyc, Nature Mater. **13**, 119 (2014).
[13] Y. Kim, W. Jeong, K. Kim, W. Lee, and P. Reddy, Nature Nanotech. **9**, 881 (2014).
[14] E.-S. Lee, S. Cho, H.-K. Lyeo, and Y.-H. Kim, Phys. Rev. Lett. **112**, 136601 (2014).
[15] R. Lake and S. Datta, Phys. Rev. B **46**, 4757 (1992).
[16] M. Paulsson and S. Datta, Phys. Rev. B **67**, 241403 (2003).
[17] T. E. Humphrey and H. Linke, Phys. Rev. Lett. **94**, 096601 (2005).
[18] M. Galperin, A. Nitzan, and M. A. Ratner, Molecular Physics **106**, 397 (2008).
[19] Y.-S. Liu, Y.-R. Chen, and Y.-C. Chen, ACS Nano **3**, 3497 (2009).
[20] Y.-S. Liu and Y.-C. Chen, Phys. Rev. B **79**, 193101 (2009).
[21] Y. Dubi and M. Di Ventra, Nano Letters **9**, 97 (2009).
[22] M. Leijnse, M. R. Wegewijs, and K. Flensberg, Phys. Rev. B **82**, 045412 (2010).
[23] O. Entin-Wohlman, Y. Imry, and A. Aharony, Phys. Rev. B **82** (2010).
[24] J. Fransson and M. Galperin, Phys. Chem. Chem. Phys. **13**, 14350 (2011).
[25] Y.-S. Liu, B. C. Hsu, and Y.-C. Chen, The Journal of Physical Chemistry C **115**, 6111 (2011).
[26] Y. Dubi and M. Di Ventra, Rev. Mod. Phys. **83**, 131 (2011).
[27] O. Entin-Wohlman and A. Aharony, Phys. Rev. B **85**, 085401 (2012).
[28] B. K. Nikolić, K. K. Saha, T. Markussen, and K. S. Thygesen, Journal of Computational Electronics **11**, 78 (2012).
[29] D. Sánchez and R. López, Phys. Rev. Lett. **110**, 026804 (2013).
[30] M. Esposito, K. Lindenberg, and C. Van den Broeck, Phys. Rev. Lett. **102**, 130602 (2009).
[31] B. Rutten, M. Esposito, and B. Cleuren, Phys. Rev. B **80**, 235122 (2009).
[32] Esposito, M., Lindenberg, K., and Van den Broeck, C., EPL **85**, 60010 (2009).
[33] M. Esposito, R. Kawai, K. Lindenberg, and C. Van den Broek, Phys. Rev. E **81**, 041106 (2010).
[34] M. Esposito, N. Kumar, K. Lindenberg, and C. Van den Broeck, Phys. Rev. E **85**, 031117 (2012).
[35] N. Nakpathomkun, H. Q. Xu, and H. Linke, Phys. Rev. B **82**, 235428 (2010).
[36] B. Cleuren, B. Rutten, and C. Van den Broeck, Phys. Rev. Lett. **108**, 120603 (2012).
[37] O. Abah, J. Roßnagel, G. Jacob, S. Deffner, F. Schmidt-Kaler, K. Singer, and E. Lutz, Phys. Rev. Lett. **109**, 203006 (2012).
[38] A. Thess, Phys. Rev. Lett. **111**, 110602 (2013).
[39] K. Brandner, K. Saito, and U. Seifert, Phys. Rev. Lett. **110**, 070603 (2013).
[40] K. Brandner and U. Seifer, New Journal of Physics **15**, 105003 (2013).
[41] R. S. Whitney, Phys. Rev. Lett. **112**, 130601 (2014).
[42] J. Roßnagel, O. Abah, F. Schmidt-Kaler, K. Singer, and E. Lutz, Phys. Rev. Lett. **112**, 030602 (2014).
[43] L. Arrachea, N. Bode, and F. von Oppen, Phys. Rev. B **90**, 125450 (2014).
[44] C. Jarzynski, Annual Review of Condensed Matter Physics **2**, 329 (2011).
[45] U. Seifert, Rep. Prog. Phys. **75**, 126001 (2012).
[46] C. Van den Broeck and M. Esposito, Physica A **418**, 6 (2015).
[47] K. Sekimoto, *Stochastic Energetics* (Springer, 2010).
[48] G. Verley, M. Esposito, T. Willaert, and C. Van den Broeck, Nature Commun. **5**, 4721 (2014).
[49] G. Verley, T. Willaert, C. Van den Broeck, and M. Esposito, Phys. Rev. E **90**, 052145 (2014).
[50] M. Polettini, G. Verley, and M. Esposito, Phys. Rev. Lett. **114**, 050601 (2014).
[51] T. R. Gingrich, G. M. Rotskoff, S. Vaikuntanathan, and P. L. Geissler, New J. Phys. **16**, 102003 (2014).
[52] S. Rana, P. Pal, A. Saha, and A. M. Jayannavar, Phys. Rev. E **90**, 042146 (2014).
[53] K. Proesmans, B. Cleuren, and C. Van den Broeck, arXiv: 1411.3531 (2014).
[54] I. A. Martínez, E. Roldán, L. Dinis, D. Petrov, J. M. P. Parrondo, and R. Rica, arXiv: 1412.1282 (2014).
[55] Z. Qian, R. Li, X. Zhao, S. Hou, and S. Sanvito, Phys. Rev. B **78**, 113301 (2008).
[56] O. Karlström, H. Linke, G. Karlström, and A. Wacker, Phys. Rev. B **84**, 113415 (2011).
[57] A. J. White, B. D. Fainberg, and M. Galperin, J. Phys. Chem. Lett. **3**, 2738 (2012).
[58] U. Peskin and M. Galperin, J. Chem. Phys. **136**, 044107 (2012).
[59] M. Galperin and A. Nitzan, J. Phys. Chem. B **117**, 4449 (2013).
[60] A. J. White, U. Peskin, and M. Galperin, Phys. Rev. B **88**, 205424 (2013).
[61] C. Patoux, C. Coudret, J.-P. Launay, C. Joachim, and A. Gourdon, Inorg. Chem. **36**, 5037 (1997).
[62] M. Mayor, H. B. Weber, J. Reichert, M. Elbing, C. von Hänisch, D. Beckmann, and M. Fischer, Ang. Chim. Int. Ed. **47**, 5834 (2003).
[63] H. Lee, Y.-C. Cheng, and G. R. Fleming, Science **316**, 1462 (2007).
[64] G. S. Engel, T. R. Calhoun, E. L. Read, T.-K. Ahn, T. Mancal, Y.-C. Cheng, R. E. Blankenship, and G. R. Fleming, Nature **446**, 782 (2007).
[65] R. Härtle, M. Butzin, O. Rubio-Pons, and M. Thoss, Phys. Rev. Lett. **107**, 046802 (2011).
[66] H. Vazquez, R. Skouta, S. Schneebeli, M. Kamenetska, R. Breslow, L. Venkataraman, and M. Hybertsen, Nature Nanotech. **7**, 663 (2012).
[67] L. S. Levitov, H. Lee, and G. B. Lesovik, J. Math. Phys.

37, 4845 (1996).
[68] Y. Utsumi, D. S. Golubev, and G. Schön, Phys. Rev. Lett. **96**, 086803 (2006).
[69] A. O. Gogolin and A. Komnik, Phys. Rev. B **73**, 195301 (2006).
[70] K. Schönhammer, Phys. Rev. B **75**, 205329 (2007).
[71] M. Esposito, U. Harbola, and S. Mukamel, Rev. Mod. Phys. **81**, 1665 (2009).
[72] K. Schönhammer, Journal of Physics: Condensed Matter **21**, 495306 (2009).
[73] C. Emary, Phys. Rev. B **80**, 235306 (2009).
[74] Y. Utsumi, D. S. Golubev, M. Marthaler, K. Saito, T. Fujisawa, and G. Schön, Phys. Rev. B **81**, 125331 (2010).
[75] J. Fransson and M. Galperin, Phys. Rev. B **81**, 075311 (2010).
[76] M. Esposito and M. Galperin, J. Phys. Chem. C **114**, 20362 (2010).
[77] T.-H. Park and M. Galperin, Phys. Rev. B **84**, 205450 (2011).
[78] Y. Utsumi, O. Entin-Wohlman, A. Ueda, and A. Aharony, Phys. Rev. B **87**, 115407 (2013).
[79] M. Esposito and K. Lindenberg, Phys. Rev. E **77**, 051119 (2008).
[80] R. Sanchez and M. Büttiker, EPL **100**, 47008 (2012).
[81] R. Sánchez and M. Büttiker, Phys. Rev. B **83**, 085428 (2011).
[82] L. Simine and D. Segal, Phys. Chem. Chem. Phys. **14**, 13820 (2012).
[83] G. Schaller, T. Krause, T. Brandes, and M. Esposito, New Journal of Physics **15**, 033032 (2013).
[84] P. Wollfarth, A. Shnirman, and Y. Utsumi, Phys. Rev. B **90**, 165411 (2014).
[85] M. Leijnse and M. R. Wegewijs, Phys. Rev. B **78**, 235424 (2008).
[86] M. Esposito and M. Galperin, Phys. Rev. B **79**, 205303 (2009).
[87] D. Djukic and J. M. van Ruitenbeek, Nano Lett. **6**, 789 (2006).
[88] M. Kiguchi, O. Tal, S. Wohlthat, F. Pauly, M. Krieger, D. Djukic, J. C. Cuevas, and J. M. van Ruitenbeek, Phys. Rev. Lett. **101**, 046801 (2008).
[89] O. Tal, M. Krieger, B. Leerink, and J. M. van Ruitenbeek, Phys. Rev. Lett. **100**, 196804 (2008).
[90] M. Kumar, R. Avriller, A. L. Yeyati, and J. M. van Ruitenbeek, Phys. Rev. Lett. **108**, 146602 (2012).
[91] N. L. Schneider, J. T. Lü, M. Brandbyge, and R. Berndt, Phys. Rev. Lett. **109**, 186601 (2012).
[92] R. Chen, P. J. Wheeler, and D. Natelson, Phys. Rev. B **85**, 235455 (2012).
[93] M. Esposito, U. Harbola, and S. Mukamel, Phys. Rev. B. **75**, 155316 (2007).
[94] D. Bernard and B. Doyon, J. Phys. A **45**, 362001 (2012).
[95] F. Zhan, S. Denisov, and P. Hanggi, Phys. Stat. Sol. (b) **250**, 2355 (2013).
[96] F. Battista, F. Haupt, and J. Splettstoesser, Phys. Rev. B **90**, 085418 (2014).
[97] M. Marcus and H. Minc, *Introduction to Linear Algebra* (Dover Publications, Inc., New York, 1988).